Abiotic synthesis of purine and pyrimidine ribonucleosides in aqueous microdroplets

Inho Nam[a,b], Hong Gil Nam[a,c,1], and Richard N. Zare[b,1]

[a]Center for Plant Aging Research, Institute for Basic Science, Daegu 42988, Republic of Korea; [b]Department of Chemistry, Stanford University, Stanford, CA 94305; and [c]Department of New Biology, Daegu Gyeongbuk Institute of Science and Technology (DGIST), Daegu 42988, Republic of Korea

Aqueous microdroplets (<1.3 μm in diameter on average) containing 15 mM D-ribose, 15 mM phosphoric acid, and 5 mM of a nucleobase (uracil, adenine, cytosine, or hypoxanthine) are electrosprayed from a capillary at +5 kV into a mass spectrometer at room temperature and 1 atm pressure with 3 mM divalent magnesium ion (Mg^{2+}) as a catalyst. Mass spectra show the formation of ribonucleosides that comprise a four-letter alphabet of RNA with a yield of 2.5% of uridine (U), 2.5% of adenosine (A), 0.7% of cytidine (C), and 1.7% of inosine (I) during the flight time of ~50 μs. In the case of uridine, no catalyst is required. An aqueous solution containing guanine cannot be generated under the same conditions given the extreme insolubility of guanine in water. However, inosine can base pair with cytidine and thus substitute for guanosine. Thus, a full set of ribonucleosides to generate the purine–pyrimidine base pairs A-U and I-C are spontaneously generated in aqueous microdroplets under similar mild conditions.

microdroplet chemistry | origin of life | prebiotic chemistry | purine ribonucleosides | pyrimidine ribonucleosides

One hypothesis concerning the origin of life postulates an RNA world that existed on Earth before modern cells arose (1). According to this hypothesis, RNA stored genetic information and catalyzed chemical reactions in primitive cells (2, 3). However, a major missing link has been how to construct from simpler molecules the ribonucleosides, which are the building blocks of RNA (1–3). This challenge seems quite daunting because the making of ribonucleosides in a water solution from ribose and some suitable nucleobase, such as the purines adenine and guanine, and the pyrimidines uracil and cytosine, is thermodynamically uphill (4, 5). Recently, possible routes for the prebiotic synthesis of purine and pyrimidine ribonucleosides were studied by bypassing the biological synthesis mechanism (5–8). These routes demand different environments, although it might be more favorable if purine and pyrimidine ribonucleosides could be condensed in the same environment for the fabrication of RNA. Moreover, these mechanisms require complex, sequential reactions with reaction times in the range of days, which may make them less relevant for creating a prebiotic chemistry in which RNA could develop. As described below, we present an alternative route for the synthesis of ribonucleosides that seems to be sufficiently mild and general that it might have played a role in turning simpler molecules into biomolecules.

In cells, the synthesis of ribonucleosides takes two paths: nucleotide metabolism and the salvage pathway (9–11). In nucleotide metabolism, 5-phosphoribosyl-1-pyrophosphate (PRPP) formed from D-ribose-5-phosphate (Rib-5-P) and nucleobases are changed into a ribonucleotide and two phosphates (9). As part of the salvage pathway, Rib-1-P and a nucleobase are transformed into a ribonucleoside and a phosphate (9–11), as illustrated in Fig. 1. The salvage pathway in vivo is a reaction in which ribonucleosides are synthesized from organic intermediates. Specifically, Rib-1-P is added to a free nucleobase by a phosphorylase enzyme to form a ribonucleoside. The most important part of both reactions is that a carbon atom at the first position (C1) in ribose links to the nucleobase.

In a recent study, we showed a synthetic pathway for the formation of Rib-1-P using aqueous, high–surface-area microdroplets. This surface or near-surface reaction circumvents the fundamental thermodynamic problem of the condensation reaction (12). It has been suggested that the air–water interface provides a favorable environment for the prebiotic synthesis of biomolecules (12–17). Using the Rib-1-P made in the above abiotic manner and the salvage pathway shown in Fig. 1, we successfully generated uridine (U) (12), one of the pyrimidine ribonucleosides, in aqueous microdroplets. However, we did not investigate whether this process represents a general abiotic pathway for the generation of both purine and pyrimidine ribonucleosides. Here, we show the abiotic generation of the ribonucleosides adenosine (A), cytidine (C), and inosine (I) by surmounting the thermodynamic barrier for these reactions at or near the surface of room-temperature water microdroplets. Guanine is practically insoluble in water, which precludes the generation of aqueous microdroplets containing guanine (18). Nevertheless, inosine (I) can base pair with cytidine (C), and thus the full base pairs of ribonucleosides can be synthesized and survive under the same prebiotic conditions. In the microdroplets, a small concentration of divalent magnesium ion (Mg^{2+}), one of the main elements of Earth's crust (19), serves to catalyze the process. Because mists, clouds, and sprays are thought to be common on early Earth, these findings provide a possible missing link as to how the RNA world came about.

Significance

Discovery of an improved prebiotic method for the synthesis of ribonucleosides provides support to theories that posit a central role for RNA in the origin of life. It has been assumed that ribonucleosides arose through an abiotic process in which ribose and nucleobases became conjoined, but the direct condensation of nucleobases with ribose to give ribonucleosides in bulk solution is thermodynamically uphill. We show a general synthetic path for ribonucleosides, both purine and pyrimidine bases, using an abiotic salvage pathway in a microdroplet environment with divalent magnesium ion (Mg^{2+}) as a catalyst. Purine and pyrimidine ribonucleosides are formed simultaneously under the same conditions, which suggests a possible scenario for the spontaneous production of random ribonucleosides necessary to generate various types of primitive RNA.

[1]To whom correspondence may be addressed. Email: nam@dgist.ac.kr or zare@stanford.edu.

This article contains supporting information online at www.pnas.org/lookup/suppl/doi:10.1073/pnas.1718559115/-/DCSupplemental.
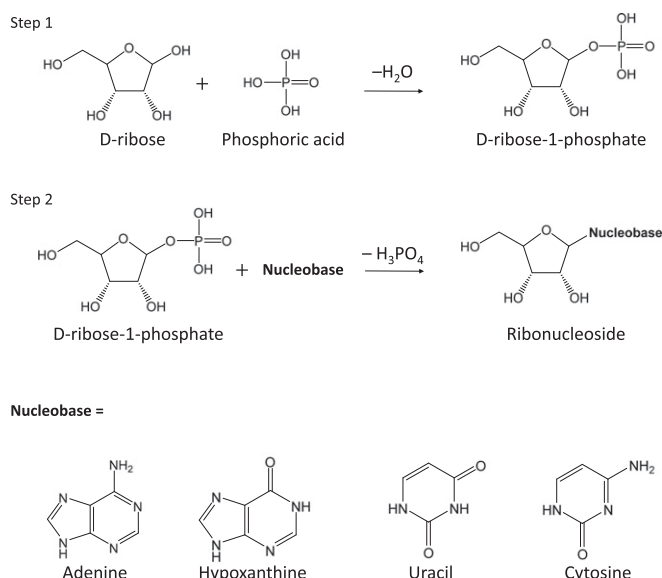
Step 1

D-ribose + Phosphoric acid $\xrightarrow{-H_2O}$ D-ribose-1-phosphate

Step 2

D-ribose-1-phosphate + **Nucleobase** $\xrightarrow{-H_3PO_4}$ Ribonucleoside

Nucleobase =

Adenine   Hypoxanthine   Uracil   Cytosine

Fig. 1. Reaction mechanism for the prebiotic synthesis of ribonucleosides by an abiotic salvage pathway using Rib-1-P as the intermediate.

Results

Generation of Aqueous Microdroplets Containing Precursors. We performed reactions to generate ribonucleosides by the abiotic salvage pathway in aqueous microdroplets (Fig. 1). The microdroplets contained 15 mM D-ribose; 15 mM phosphoric acid; and 5 mM adenine, cytosine, or hypoxanthine, which were all in deionized water. Studies were carried out in the presence of the divalent magnesium ion (3 mM Mg^{2+}). Microdroplets were generated from bulk solution with a nebulizing gas (dry N_2) at

120 psi using an electrospray ionization (ESI) source placed in front of a high-resolution mass spectrometer, as shown in Fig. S1 (20). The microdroplets traveled 5 mm at room temperature and atmospheric pressure before the reaction was stopped upon entering the heated inlet of a mass spectrometer (21). Under these conditions, a corresponding reaction time was estimated to be ~50 µs on the basis of the droplet speed (~100 m/s) (22, 23). The droplets were positively charged by external application of a potential of +5 kV to the ESI source. When a high electric field is applied to droplets, the electric charge makes an electrical force inside the droplets, which generates a droplet explosion into very fine microdroplets (Coulomb explosion) (24). Therefore, the external charge mainly affects the size of droplets, and the size of droplets controls the yield of ribonucleosides in aqueous microdroplets. Here, the sizes of droplets were observed to be, on average, <1.3 µm in diameter (Fig. S2), as determined optically (25). Without application of the external potential, the average diameter of droplets is 12.5 µm, which means the volume of droplets is at least three orders of magnitude larger than that with the external voltage. The significantly smaller surface-to-volume ratio is one of the main reasons that production of ribonucleosides was reduced in uncharged microdroplets (Fig. S2). We also checked the mass spectra of the products in microdroplets by using the above experimental scheme without Mg^{2+}. We found peaks for the mass of precursors D-ribose, phosphoric acid, and a nucleobase, such as $m/z = 136.061$ for protonated adenine, $m/z = 112.050$ for protonated cytosine, $m/z = 137.046$ for protonated hypoxanthine, and $m/z = 231.026$ for Rib-1-P, as shown in Fig. S3. However, the ribonucleosides adenosine, cytidine, and inosine were not detected in microdroplets under these conditions.

Thermodynamic Considerations Concerning Ribonucleoside Generation in Aqueous Microdroplets. To determine the reaction barrier, we present the free energy diagrams for the abiotic salvage pathways of adenosine, cytidine, inosine, and uridine showing the changes of
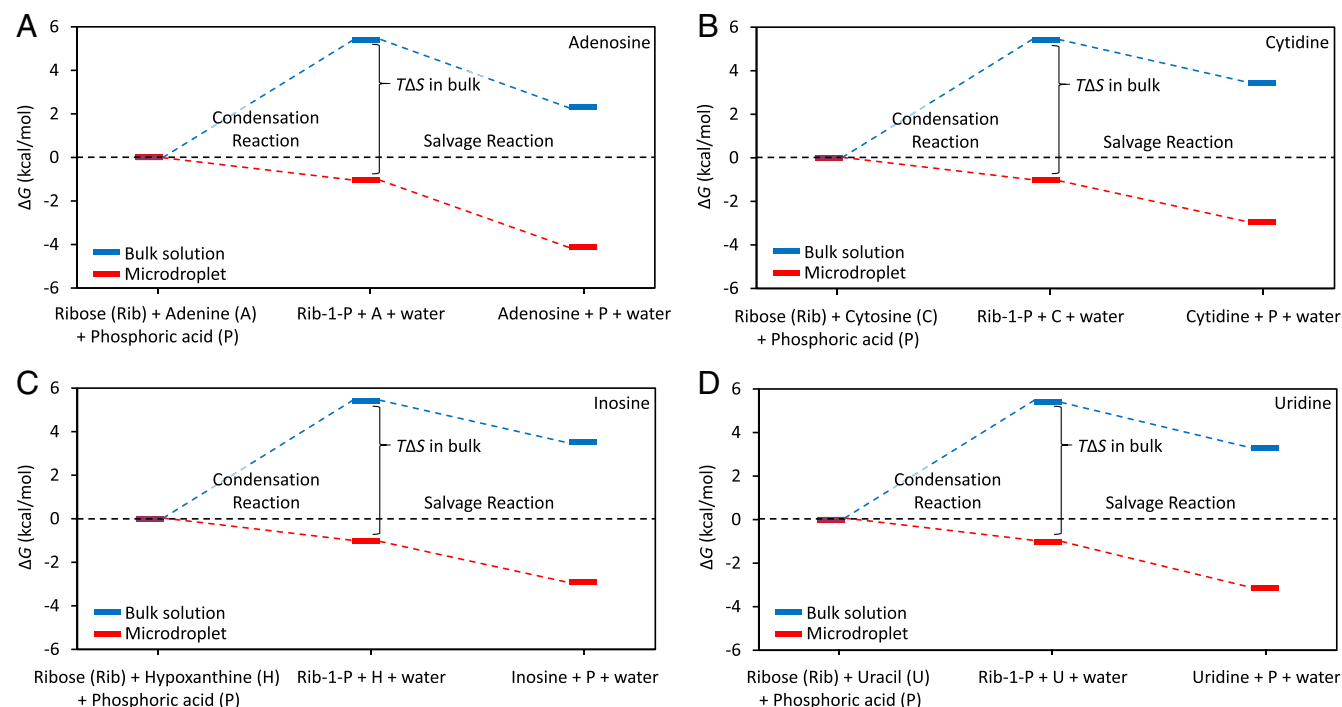

Fig. 2. Free energy diagrams for the abiotic synthesis of the ribonucleosides (A) adenosine, (B) cytidine, (C) inosine, and (D) uridine. The condensation occurs between ribose and phosphoric acid to generate Rib-1-P. The salvage reaction occurs between Rib-1-P and nucleobase to generate the corresponding ribonucleoside. The ΔG values in bulk solution (blue lines) are positive, whereas in microdroplets (red lines) they are negative.
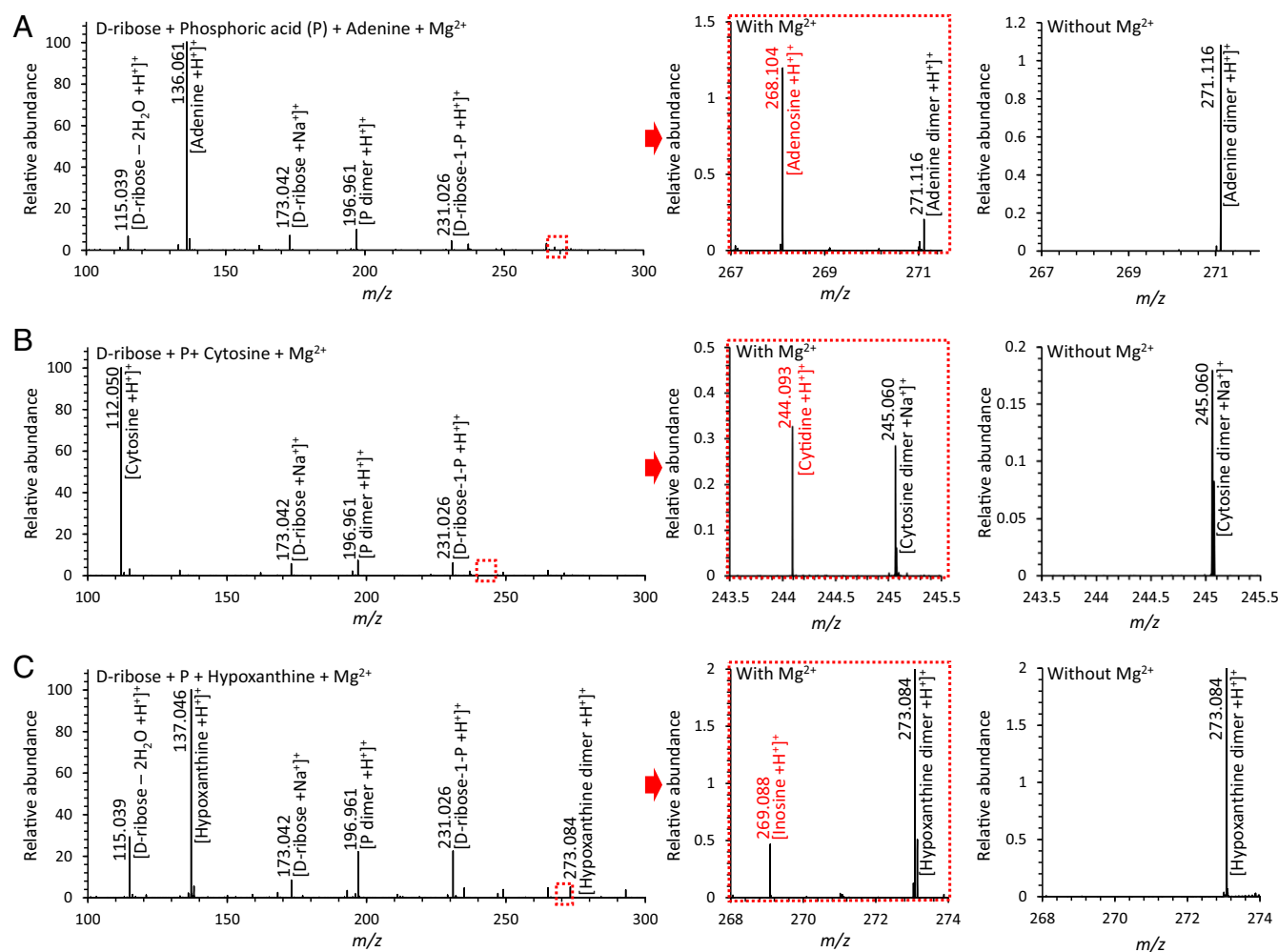
Fig. 3. Mass spectra of reactions in microdroplets containing 15 mM D-ribose, 15 mM phosphoric acid, and 5 mM of the nucleobase (*A*) adenine, (*B*) cytosine, and (*C*) hypoxanthine, with and without 3 mM Mg^{2+}. The red boxes show the detected ion signals of ribonucleosides with the Mg^{2+} catalyst, and the red letters denote the detected *m/z* peaks of (*A*) adenosine, (*B*) cytidine, and (*C*) inosine.

Gibbs free energy, ΔG, in which the data are based on previous studies (12, 26, 27) (Fig. 2). For cytidine, the ΔG value of the salvage reaction is calculated by density functional theory (DFT) using the projector-augmented wave method. The DFT calculation considers unsolvated reactants and products; however, we already observed that the calculated value is very close to the real value for the reaction in aqueous microdroplets (12). In bulk aqueous solution, a condensation reaction between ribose and phosphate has a large negative value of $T\Delta S$ (−6.3 kcal/mol) or $\Delta S = -2.1 \times 10^{-2}$ kcal/mol·K, which results in a positive Gibbs free energy change ($\Delta G = +5.4$ kcal/mol) (12, 27). However, in bulk solution reactions between phosphate in Rib-1-P and adenine, cytosine, or hypoxanthine following a salvage pathway, the values of ΔG are negative: −3.1, −1.94, and −1.88 kcal/mol, respectively (26, 27). It appears that the salvage reaction between Rib-1-P and nucleobase, both purine and pyrimidine, can occur spontaneously once Rib-1-P is formed as an intermediate. This is in good agreement with uridine fabrication by a salvage pathway, which also has a negative ΔG value, −2.13 kcal/mol (28). Combining this information, we find that syntheses of adenosine, cytidine, inosine, and uridine all have positive ΔG values, +2.30, +3.46, +3.52 and +3.27 kcal/mol, respectively (blue lines in Fig. 2), in bulk aqueous solution.

In sharp contrast to the thermodynamic inhibition of ribose phosphorylation in bulk solution ($\Delta G = +5.4$ kcal/mol), we have

shown that the synthesis of Rib-1-P from ribose and phosphoric acid in microdroplets has a ΔG value of −1.1 kcal/mol (12). We previously demonstrated that the phosphorylation of ribose in microdroplets displays a negligible change of entropy ($\Delta S = 7 \times 10^{-4}$ kcal/mol·K). Therefore, microdroplets alter the kinetics and thermodynamics of ribose phosphorylation. The decreased entropic change for this chemical reaction in microdroplets compared with bulk solution could be attributed to the molecular organization and alignment of reactants at the air–water interface of microdroplet surfaces (29). Consequently, the ΔG values for the synthesis of the ribonucleosides adenosine, cytidine, inosine, and uridine become negative in microdroplets: −4.12, −2.96, −2.90, and −3.15 kcal/mol, respectively (red lines in Fig. 2). These results indicate that the reaction to generate both purine and pyrimidine ribonucleosides becomes thermodynamically allowed in microdroplets based on the salvage pathway. Of course, this condition is necessary but not sufficient for the formation of the purine and pyrimidine ribonucleosides. We must also examine the kinetics of these reactions.

Mg^{2+} Catalytic Effect for Ribonucleoside Generation. The thermodynamic feasibility of the abiotic salvage reaction suggests that the lack of ribonucleoside production for adenosine, cytidine, and inosine in microdroplets (Fig. S4) is the consequence of poor kinetics. To accelerate the kinetics of the ribonucleoside
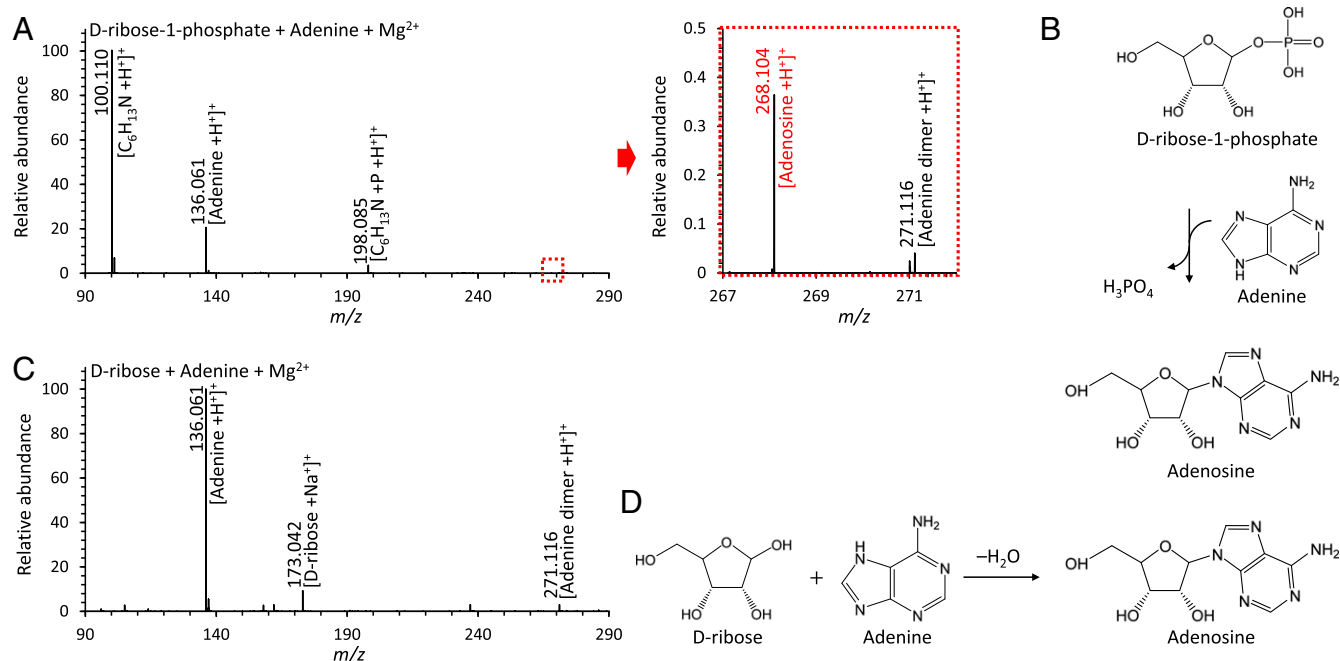
Fig. 4. The synthetic path of adenosine in microdroplets with Mg^{2+} catalyst. (*A*) Mass spectra for the products of reaction between adenine and Rib-1-P and (*B*) the mechanism of salvage reaction between adenine and Rib-1-P to give adenosine. Red letters denote the detected *m/z* peak of the adenosine from an abiotic salvage reaction. (*C*) Mass spectrum for the products of reaction between D-ribose and adenine in the absence of phosphate and (*D*) the previously assumed mechanism for the direct ribosylation of adenine. $C_6H_{13}N$ and P denote a fragment of adenine (cyclohexylamine) and phosphoric acid.

generation, we investigated the use of different metal ion catalysts, including Mg^{2+}, Ca^{2+}, and Fe^{2+}. We found that 3 mM Mg^{2+} in microdroplets worked well. In previous research, Mg^{2+} was also needed with inorganic polyphosphates for making adenosine using heating and drying (7). In addition, the microdroplet environment can support the acceleration of chemical reactions, in contrast to what happens in bulk solution. We and other groups have shown the acceleration property of microdroplets (10^3- to 10^6-fold higher than bulk) for various chemical reactions, such as redox reactions (20, 30), protein unfolding (21), chlorophyll demetallation (31), addition/condensation reactions (32), carbon-carbon bond-forming reactions (33), and elimination/substitution reactions (34). With Mg^{2+}, the abiotic salvage reaction in microdroplets for generation of ribonucleosides was dramatically changed. In each mass spectrum of microdroplets containing Mg^{2+} we observed additional peaks (Fig. 3) that were not present in the reactant solutions without Mg^{2+}. In particular, peaks at $m/z = 268.104$ for adenosine, $m/z = 244.089$ for cytosine, and $m/z = 269.088$ for hypoxanthine were identified as protonated adenosine $[Adenosine +H^+]^+$, protonated cytidine $[Cytidine +H^+]^+$, and protonated inosine $[Inosine +H^+]^+$, respectively. That means that ribonucleosides, both purine and pyrimidine bases, proceed spontaneously to form under these conditions in tens of microseconds at room temperature and atmospheric pressure. By ionization efficiency calibrations, the product yields for adenosine, cytosine, and inosine were determined to be ~2.5%, 0.7%, and 1.7%, respectively (Fig. S4).

We performed tandem MS using collision-induced dissociation (CID) to confirm the structure of generated molecules in the microdroplets. The fragmentation pattern for each reacted microdroplet includes a nucleobase peak, $[Adenine +H^+]^+$, $[Cytosine +H^+]^+$, or $[Hypoxanthine +H^+]^+$, which exactly matched that of the respective ribonucleoside (Fig. S5).

Discussion

Plausible Mechanism for Ribonucleoside Generation in Aqueous Microdroplets. To determine the plausible mechanism of ribonucleoside generation, we tested multiple-step reactions in microdroplets

in the presence of Mg^{2+}. First, we tested the solution containing 15 mM Rib-1-P and 5 mM adenine (Fig. 4 *A* and *B*). After generation of droplets, the adenosine was still synthesized (yield of ~4%), which means that the exchange reaction occurs between Rib-1-P and adenine in the same manner as a salvage reaction. However, from a solution containing D-ribose and adenine, there was no observation of adenosine, as shown in Fig. 4 *C* and *D*. Thus, a direct condensation reaction between ribose and adenine is negligible compared with the abiotic salvage synthesis. Understandably, Rib-1-P was readily generated from the solution, including ribose and phosphate, as shown in our previous research (Fig. S6).

Role of Mg^{2+} Catalyst. The abiotic generation of ribonucleosides occurs on the order of microseconds with the Mg^{2+} catalyst. Mg^{2+} plays important roles in biology—for example, stabilizing proteins, nucleic acids, and cell membranes, as well as serving as a cofactor for enzymes (18). We also speculate that Mg^{2+} could contribute to transition state stabilization, because Mg^{2+} appears to change the kinetics of reactions. An example of Mg^{2+} stabilizing the transition states in biochemical reactions has been reported in self-cleaving ribozymes (35). It is notable that synthesis of uridine does not require Mg^{2+}, which may provide a mechanistic insight on the role of Mg^{2+}.

Conclusions

We have provided what we believe to be a feasible prebiotic pathway to synthesize ribonucleosides, both purine and pyrimidine bases, under the same conditions of aqueous microdroplets containing small amounts of Mg^{2+}. In contrast to bulk solution, microdroplets can overcome the thermodynamic barrier for these condensation reactions. The thermodynamic change for chemical reactions in microdroplets could be attributed, in part, to the molecular organization and alignment of reactants at the air–water interface of microdroplet surfaces (36, 37). The air–water interface possesses a strong electric field, which could influence the organization of reactant molecules, as well as the kinetics and thermodynamics of chemical reactions (29). With

the unique properties of Mg^{2+} in biology, the present study suggests that the inorganic chemistry of Mg^{2+} might have a key role in the origin of life with microdroplet chemistry. It is of special importance that both purine and pyrimidine ribonucleosides are made in the same environment, which suggests the simultaneous production of large pools of random ribonucleosides in the same microdroplets that might lead (38) to the production of self-replicating RNA.

Materials and Methods

Generation of Aqueous Microdroplets Containing Precursors. The aqueous solution of 15 mM D-ribose, 15 mM phosphoric acid, and 5 mM nucleobases was injected with 3 mM magnesium sulfate by a mechanical syringe pump through a hypodermic needle to the fused silica capillary directing toward a mass spectrometer inlet. A coaxial sheath gas (dry N_2 at 120 psi) flow around the capillary results in nebulization and also helps to direct the spray emerging from the capillary tip toward the mass spectrometer inlet (the flow rate of 5 μL/min through silica tubing). A positive voltage, +5 kV, was applied to the hypodermic needle. At a mass spectrometer inlet, the reactants, intermediates, and products are released from droplets by Coulomb fission and enter into the mass spectrometer through a heated capillary. The capillary temperature was maintained at 275 °C and the capillary voltage at 44 V. To confirm the identities of synthesized ribonucleosides, tandem MS was conducted by CID. For all mass spectrometric analyses, the spray distance (the distance from spray tip to the entrance of the heated capillary) was kept at 5 mm. Mass spectra were detected by high-resolution MS (Thermo Scientific LTQ Orbitrap XL Hybrid Ion Trap-Orbitrap). All of the necessary chemicals were purchased from Sigma-Aldrich. HPLC-grade solvents were purchased from Fisher Scientific.

Quantitative Analysis. The quantitative analysis for the estimate of percentage yield of the above reactions was performed by an ionization efficiency calibration. Calibration plots were made by electric spraying the mixture of the reactant and the corresponding authentic product in known concentration ratios. As the ion signal intensities of the reactant (I_R) and the product (I_P) both depend on their concentrations and ionization efficiencies, we calculated the ratio $I_P:I_R$ and plotted it against the product-to-reactant concentration ratio ([P]:[R]). We estimated the yield of the reaction from this calibration plot.

DFT Calculations. First-principles calculations were carried out on the basis of periodic DFT using a generalized gradient approximation within the Perdew-Burke-Ernzerhof exchange correction functional (39, 40). We used the projector-augmented wave method for describing ionic cores as implemented in the Vienna ab initio simulation package (VASP) (41). The wave functions were constructed from the expansion of plane waves with an energy cutoff of 520 eV. A $6 \times 6 \times 6$ k-point mesh Monkhorst-Pack method was used to sample the Brillioun zone. The electronic optimization steps were self-consistently converged over 10^{-4} eV per formula unit.

1. Orgel LE (1998) The origin of life—A review of facts and speculations. *Trends Biochem Sci* 23:491–495.
2. Ruiz-Mirazo K, Briones C, de la Escosura A (2014) Prebiotic systems chemistry: New perspectives for the origins of life. *Chem Rev* 114:285–366.
3. Sutherland JD (2016) The origin of life–Out of the blue. *Angew Chem Int Ed Engl* 55: 104–121.
4. Orgel LE (2004) Prebiotic chemistry and the origin of the RNA world. *Crit Rev Biochem Mol Biol* 39:99–123.
5. Powner MW, Gerland B, Sutherland JD (2009) Synthesis of activated pyrimidine ribonucleotides in prebiotically plausible conditions. *Nature* 459:239–242.
6. Xu J, et al. (2017) A prebiotically plausible synthesis of pyrimidine β-ribonucleosides and their phosphate derivatives involving photoanomerization. *Nat Chem* 9:303–309.
7. Fuller WD, Sanchez RA, Orgel LE (1972) Studies in prebiotic synthesis. VI. Synthesis of purine nucleosides. *J Mol Biol* 67:25–33.
8. Becker S, et al. (2016) A high-yielding, strictly regioselective prebiotic purine nucleoside formation pathway. *Science* 352:833–836.
9. Moffatt BA, Ashihara H (2002) Purine and pyrimidine nucleotide synthesis and metabolism. *Arabidopsis Book* 1:e0018.
10. Cappiello M, Mascia L, Scolozzi C, Giorgelli F, Ipata PL (1998) In vitro assessment of salvage pathways for pyrimidine bases in rat liver and brain. *Biochim Biophys Acta* 1425:273–281.
11. Mascia L, Cappiello M, Cherri S, Ipata PL (2000) In vitro recycling of alpha-D-ribose 1-phosphate for the salvage of purine bases. *Biochim Biophys Acta* 1474:70–74.
12. Nam I, Lee JK, Nam HG, Zare RN (2017) Abiotic production of sugar phosphates and uridine ribonucleoside in aqueous microdroplets. *Proc Natl Acad Sci USA* 114: 12396–12400.
13. Walde P, Umakoshi H, Stano P, Mavelli F (2014) Emergent properties arising from the assembly of amphiphiles: Artificial vesicle membranes as reaction promoters and regulators. *Chem Commun (Camb)* 50:10177–10197.
14. Fallah-Araghi A, et al. (2014) Enhanced chemical synthesis at soft interfaces: A universal reaction-adsorption mechanism in microcompartments. *Phys Rev Lett* 112:028301.
15. Griffith EC, Vaida V (2012) In situ observation of peptide bond formation at the water-air interface. *Proc Natl Acad Sci USA* 109:15697–15701.
16. Tuck A (2002) The role of atmospheric aerosols in the origin of life. *Surv Geophys* 23: 379–409.
17. Dobson CM, Ellison GB, Tuck AF, Vaida V (2000) Atmospheric aerosols as prebiotic chemical reactors. *Proc Natl Acad Sci USA* 97:11864–11868.
18. Windholz M (1976) *The Merck Index* (Merck & Co, Inc., Kenilworth, NJ), pp 1–593.
19. Holm NG (2012) The significance of Mg in prebiotic geochemistry. *Geobiology* 10: 269–279.
20. Banerjee S, Zare RN (2015) Syntheses of isoquinoline and substituted quinolines in charged microdroplets. *Angew Chem Int Ed Engl* 54:14795–14799.
21. Lee JK, Kim S, Nam HG, Zare RN (2015) Microdroplet fusion mass spectrometry for fast reaction kinetics. *Proc Natl Acad Sci USA* 112:3898–3903.
22. Wang R, et al. (2011) The role of nebulizer gas flow in electrosonic spray ionization (ESSI). *J Am Soc Mass Spectrom* 22:1234–1241.
23. Venter A, Sojka PE, Cooks RG (2006) Droplet dynamics and ionization mechanisms in desorption electrospray ionization mass spectrometry. *Anal Chem* 78:8549–8555.
24. Bock N, Woodruff MA, Hutmacher DW, Dargaville TR (2011) Electrospraying, a reproducible method for production of polymeric microspheres for biomedical applications. *Polymers (Basel)* 3:131–149.
25. Jansson ET, Lai YH, Santiago JG, Zare RN (2017) Rapid hydrogen-deuterium exchange in liquid droplets. *J Am Chem Soc* 139:6851–6854.
26. Mascia L, Cotrufo T, Cappiello M, Ipata PL (1999) Ribose 1-phosphate and inosine activate uracil salvage in rat brain. *Biochim Biophys Acta* 1472:93–98.
27. Camici M, Sgarrella F, Ipata PL, Mura U (1980) The standard Gibbs free energy change of hydrolysis of alpha-D-ribose 1-phosphate. *Arch Biochem Biophys* 205:191–197.
28. SI International (2016) MetaCyc Reaction: 2.4.2.2/2.4.2.3. Available at https://biocyc.org/meta/new-image?type=reaction&object=urphos-rxn. Accessed September 6, 2017.
29. Kathmann SM, Kuo I-FW, Mundy CJ (2008) Electronic effects on the surface potential at the vapor-liquid interface of water. *J Am Chem Soc* 130:16556–16561.
30. Lee JK, Banerjee S, Nam HG, Zare RN (2015) Acceleration of reaction in charged microdroplets. *Q Rev Biophys* 48:437–444.
31. Lee JK, Nam HG, Zare RN (2017) Microdroplet fusion mass spectrometry: Accelerated kinetics of acid-induced chlorophyll demetallation. *Q Rev Biophys* 50:1–7.
32. Girod M, Moyano E, Campbell DI, Cooks RG (2011) Accelerated bimolecular reactions in microdroplets studied by desorption electrospray ionization. *Chem Sci (Camb)* 2:501–510.
33. Müller T, Badu-Tawiah A, Cooks RG (2012) Accelerated carbon-carbon bond-forming reactions in preparative electrospray. *Angew Chem Int Ed Engl* 51:11832–11835.
34. Yan X, Bain RM, Cooks RG (2016) Organic reactions in microdroplets: Reaction acceleration revealed by mass spectrometry. *Angew Chem Int Ed Engl* 55:12960–12972.
35. Shechner DM, et al. (2009) Crystal structure of the catalytic core of an RNA-polymerase ribozyme. *Science* 326:1271–1275.
36. Donaldson DJ, Vaida V (2006) The influence of organic films at the air-aqueous boundary on atmospheric processes. *Chem Rev* 106:1445–1461.
37. Tervahattu H, et al. (2005) Fatty acids on continental sulfate aerosol particles. *J Geophys Res* 110:D06207.
38. Bartel DP, Szostak JW (1993) Isolation of new ribozymes from a large pool of random sequences. *Science* 261:1411–1418.
39. Kresse G, Furthmüller J (1996) Efficient iterative schemes for ab initio total-energy calculations using a plane-wave basis set. *Phys Rev B Condens Matter* 54: 11169–11186.
40. Perdew JP, Burke K, Ernzerhof M (1996) Generalized gradient approximation made simple. *Phys Rev Lett* 77:3865–3868.
41. Blöchl PE (1994) Projector augmented-wave method. *Phys Rev B Condens Matter* 50: 17953–17979.